

Optimal Path Planning in Distinct Topo-Geometric Classes using Neighborhood-augmented Graph and its Application to Path Planning for a Tethered Robot in 3D

Alp Sahin and Subhrajit Bhattacharya

Abstract—Many robotics applications benefit from being able to compute multiple locally optimal paths in a given configuration space. Examples include path planning for of tethered robots with cable-length constraints, systems involving cables, multi-robot topological exploration & coverage, and, congestion reduction for mobile robots navigation without inter-robot coordination. Existing paradigm is to use topological path planning methods that can provide optimal paths from distinct topological classes available in the underlying configuration space. However, these methods usually require non-trivial and non-universal geometrical constructions, which are prohibitively complex or expensive in 3 or higher dimensional configuration spaces with complex topology. Furthermore, topological methods are unable to distinguish between locally optimal paths that belong to the same topological class but are distinct because of genus-zero obstacles in 3D or due to high-cost or high-curvature regions. In this paper we propose an universal and generalized approach to multi-class path planning using the concept of a novel neighborhood-augmented graph, search-based planning in which can compute paths in distinct topo-geometric classes. This approach can find desired number of locally optimal paths in a wider variety of configuration spaces without requiring any complex pre-processing or geometric constructions. Unlike the existing topological methods, resulting optimal paths are not restricted to distinct topological classes, thus making the algorithm applicable to many other problems where locally optimal and geometrically distinct paths are of interest. For the demonstration of an application of the proposed approach, we implement our algorithm to planning for shortest traversible paths for a tethered robot with cable-length constraint navigating in 3D. We perform simulations and real robot experiments to demonstrate that a tethered quad-rotor can follow the resulting paths without violating the length constraints.

Index Terms—multi-class path planning, topological path planning, augmented graph, tethered robot

I. INTRODUCTION

Mobile robots primarily rely upon optimal path planning algorithms while navigating in complex environments. These robots could be operating on land, in air or underwater to perform transportation, exploration, coverage and even manipulation tasks. Among the most common approaches for computing optimal paths is discrete graph-search based methods [1, 2, 3, 4] that utilize search algorithms such as Dijkstra's, A* and its variants [5, 6, 7, 8, 9, 10, 11, 12]. These

methods require the states of the robot and its configuration space to be abstracted as discretely represented graph at a desired resolution, on which the search algorithms can provide guarantees on the completeness and optimality depending on the type and resolution of the discrete representation.

There are robotics applications in which identifying paths from distinct homotopy classes is of particular interest. These applications include congestion reduction among a fleet of mobile robots, efficient exploration and coverage of unknown environments, navigation of tethered robots or cooperative manipulation using cable-connected robots [13, 14, 15, 16, 17, 18]. Topological path planning (TPP) methods address this interest by using *augmented graphs* (*homotopy* or *homology*) to not only represent the configuration space, but also encode and keep track of topological classes of the paths taken to reach a state [14, 13, 19, 20, 18, 21]. Research in this field primarily focuses on the design of homotopy invariants, which are quantities (elements from representations of the *fundamental group* of the configuration space) that are computable as a function of a given path. Each vertex on the augmented graph can be identified with the homotopy invariant computed using the path leading up to the vertex. Then by deploying existing graph-search algorithms, it becomes possible to find a desired number of paths in different homotopy classes, each of which are locally-optimal in their respective homotopy classes.

Existing algorithms for topological path planning require non-trivial constructions in the configuration space. These constructions become increasingly complex when the configuration space is higher dimensional and of complex topology. This is mainly because topological invariants are computed based on some representation of the obstacles in the configuration space. For 2D configuration spaces with convex obstacles these representations could be as simple as some non-intersecting rays emanating from representative points. However, in higher dimensional spaces, obstacles of more complex topology and geometry may only be represented with skeletons and hyper-surfaces which are certainly more challenging to construct. Besides, in such spaces the fundamental groups are often not freely generated, and hence the computation of the homotopy invariants require complex equivalence check algorithms [20].

A task that cannot be accomplished at all by the existing topological path planning algorithms is the computation of multiple locally optimal paths that are homotopic but geo-

Department of Mechanical Engineering and Mechanics, Lehigh University, 19 Memorial Drive West, Bethlehem, PA 18015, U.S.A., [als421, sub216]@lehigh.edu.

metrically different. Certain robotics applications might entail configuration spaces in which there exists limited number of topological classes, and the existing algorithms, by nature, can only return a unique path in each distinct class. Some examples include mobile robots travelling on curved terrain, or aerial robots flying around prismatic obstacles (genus-0), where all the paths in the underlying configuration space belong to a single topological class. When the task is to efficiently explore around a high curvature landform (a hill or a valley) or navigate around obstacles while remaining tethered to a base, robots will benefit from being able to distinguish between locally optimal and geometrically distinct paths. Unlike topologically distinct paths, they can be continuously deformed into each other but only under significant increases and decreases in length (stretch and compression) during the deformation.

The topo-geometric path planning approach proposed in this paper enables computation of multiple locally optimal paths while remaining scalable to higher dimensional and complex configuration spaces. This is accomplished by constructing and comparing neighborhoods around locally optimal paths leading upto vertices on the search graph. Within every run of the search algorithm, we perform smaller sub-searches on the existing graph starting from vertices in the open list. Every sub-search is performed for a fixed depth and the resulting subgraph constitutes the neighborhood for the vertex. By augmenting the graph with these neighborhood sets and using available graph-search algorithms, it becomes possible to find desired number of paths, each of which are locally optimal in the underlying configuration space without requiring any further constructions. These paths are guaranteed to be geometrically distinct, but they could also be topologically distinct depending on the topology of the configuration space.

The contributions of this paper are as follows:

- Design of a novel topo-geometric path planning algorithm that uses a *neighborhood augmented graph*, the construction of which is simple and does not require complex geometric constructions on the underlying configuration space.
- Demonstration of the multi-class path planning capabilities of the algorithm in 2D and 3D configuration spaces of various topologies and cost functions (including cost functions and geometries that give rise to multiple locally optimal classes of paths / geodesics even though they belong to the same topological class).
- Analysis of the performance of the proposed algorithm under various geometric conditions.
- A further generalization/modification to the proposed method for computing locally-optimal paths in environments with extremely low curvature or cost variation that would otherwise not give rise to multiple *branches* during the search in the neighborhood-augmented graph.
- Implementation of the algorithm in path planning for a tethered robot navigating in 3D and with a tether-length constraint.
- Simulations and real robot experiments featuring a teth-

ered robot to demonstrate length constrained planning capabilities across variety of environments and scenarios.

II. TECHNICAL BACKGROUND, RELATED LITERATURE AND PROBLEM MOTIVATION

A. Discrete Path Planning Algorithms

Discrete search based path planning has been used extensively in solving motion planning problems in robotics because of its simplicity, effectiveness and efficiency [1, 2, 3, 4]. It involves an incremental and on-the-fly construction of a discrete representation of a configuration space (usually a graph representation that is created systematically or through sampling, or a simplicial complex representation), and exploration of the discrete representation using a search algorithm from a start state until a target or goal state is reached. Traditional graph search algorithms such as Dijkstra's [5], A* [6] and D* [7] construct and explore a configuration graph in a systematic manner, while algorithms such as PRM [8] and RRT [9] use sampling based construction and randomized search approaches. In recent years development of any-angle search algorithms [10, 11] have allowed computation of optimal paths that are not necessarily restricted to a graph, and development of search algorithms for simplicial complex representations (instead of graph representations) have allowed computation of smooth paths that are optimal in the underlying configuration space [12].

B. Prior Work: Topological Path Planning – Homotopy Invariants and Homotopy-augmented Graph

The main theoretical and algorithmic contribution of this paper is to develop an algorithm for computing multiple distinct paths from a given start to a given goal point in a configuration. To motivate this work, in this section we start by introducing some related prior work on computation of multiple paths in *topologically distinct* classes in a configuration space, and discuss some of its applications. For more details on this topic, the reader can refer to the author's prior work on topological path planning [14, 13, 19, 20, 18].

Definition 1 (Homotopy Classes of Paths). *Two paths connecting the same start and goal points in a configuration space are said to be in the same homotopy class (or homotopic) if one can be continuously deformed into another (without intersecting/crossing obstacles (Figure 1a). Otherwise they are called non-homotopic.*

Homotopy classes are the main topological classes of interest when it comes to paths or trajectories in a configuration space. A *homotopy invariant* is a quantitative measure of homotopy classes, which is a function of paths in the configuration space, and is represented as $h(\gamma)$ for a path γ . The construction of such homotopy invariants require geometric constructions in the configuration space (for example, non-intersecting rays emanating from obstacles in planar domains, or surfaces bounded by obstacles in spatial domains – Figures 1b,1c). Homotopy invariants can be incorporated in constructing discrete search graphs called *h-augmented graphs*,

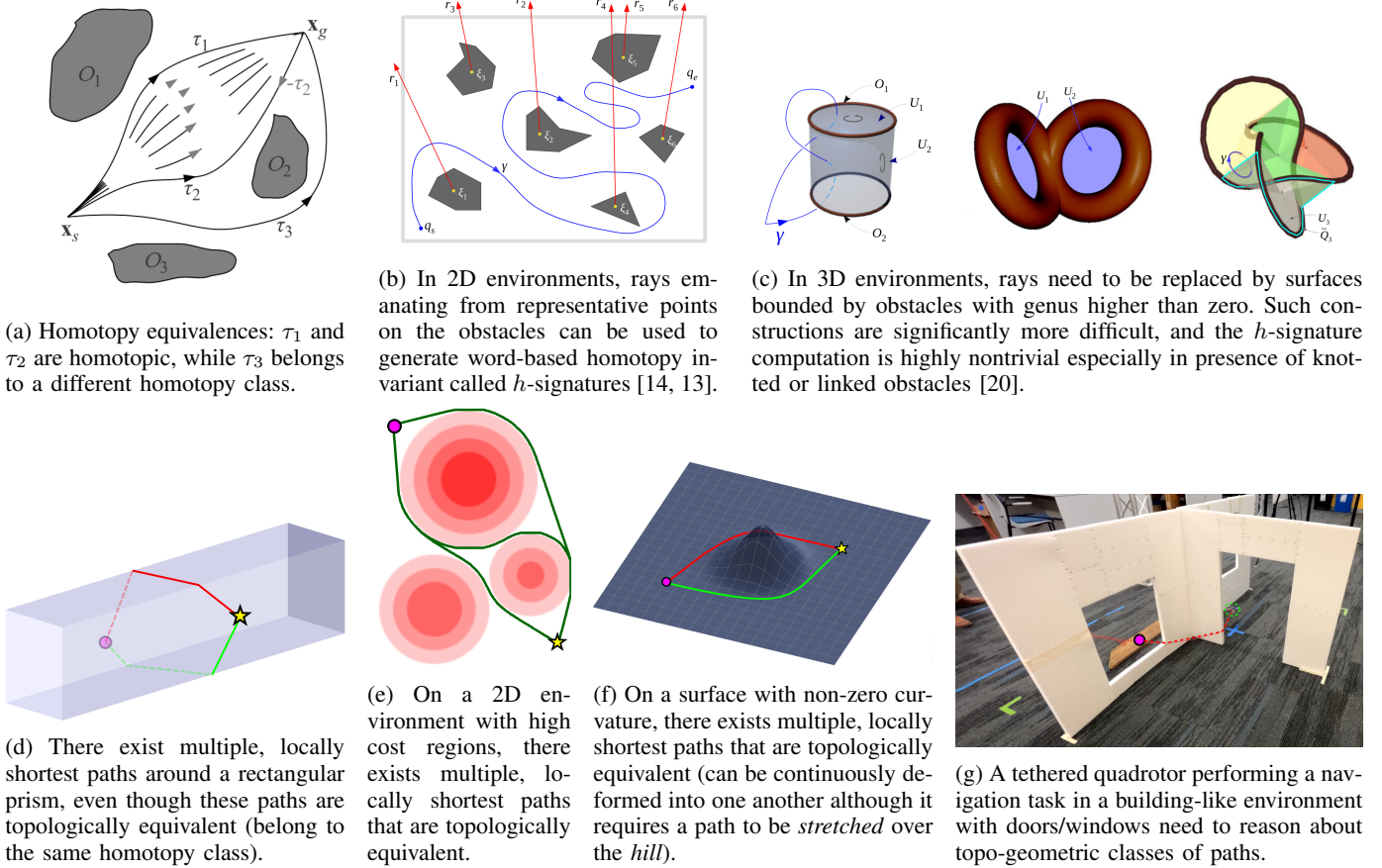


Fig. 1: **Background and Motivation** – *Top row (a-c):* Existing/prior work on *topological path planning (TPP)* for computing optimal paths in different homotopy classes. The constructions and computations gets significantly harder in 3-D configuration spaces, requiring complex group-theoretic reasoning in presence of obstacles that are knotted or linked (such structures are encountered in urban structures such as buildings with stairways, doors and windows). *Bottom row (d-g):* Motivation behind current work – Even in absence of topologically-distinct classes of paths, there can exist different geometrically-distinct classes of paths (d-e). This, along with the increased complexity of TPP in 3D (c), motivates our current topo-geometric planning algorithm that creates an unified framework for computing multiple locally-optimal paths connecting a start and a goal configuration.

and search-based planning algorithms can be employed for computing (locally) shortest path in different homotopy classes using a process referred to as *topological path planning (TPP)*.

Some of the applications of the ability to compute locally shortest paths in distinct topological classes enabled by TPP include path planning for tethered robot with cable length constraints [13], object separation using a cable attached to two robots at its ends [14], workspace & motion planning for a multiple-cable controlled robot [15], and multi-agent path planning with topological reasoning where agents distribute in an environment based on the available topological classes [16, 17, 18].

C. Locally-optimal Paths

In this section we formalize the notion of *locally-optimal paths* (also referred to as geodesic paths) and make some key observations about them.

Definition 2 (Locally-optimal or Geodesic Paths [22]). *A path connecting a fixed pair of start and goal points in a path metric space (a space along with a cost/length function for measuring the cost/length of a path) is called locally optimal or geodesic if any small (infinitesimal) perturbation to the path results in an increase in the cost of the path.*

We first observe that given a start and a goal point in a configuration space, there can be multiple distinct geodesics connecting them that may or may not be in different homotopy classes (Figure 1). The presence of distinct homotopy classes give rise to distinct geodesic paths (at least one in each homotopy class) [23]. But even within the same homotopy class there can be multiple geodesic paths created due to geometry, curvature and non-uniform cost.

Remark 1 (Key Observation about Targets to Geodesics). *Two distinct geodesic paths connecting the same start and*

goal points in a configuration space have at least one point common to both the paths at which the tangents to the paths are distinct.

Usually the said common point on geodesic paths where the tangents do not match is the goal point (Figure 2(a)), q_g . However, it is possible for distinct geodesic paths to have parallel tangents at the goal, in which case there exists a point, q , on the paths earlier than the goal where the tangents are not parallel (Figure 2(b)). In that case, one can consider q to be an intermediate goal, where the tangents to the paths are distinct (and hence there are two distinct geodesic paths to q), and then the overlapping geodesic path from q to q_g simply concatenated to those distinct geodesic paths to obtain distinct geodesic paths connecting q_s and q_g .

Remark 2 (Path Neighborhoods as Proxy for Tangent Vectors). Since a reasonable representation of a tangent space of a point is a small neighborhood around the point in the configuration space, tangent vector to a path at that point can be approximately represented by a neighborhood around the path close to the point (see Figure 2). We call such a representative neighborhood a path neighborhood of the path at the point.

Motivated by these observations we provide the following definition:

Definition 3 (Topo-geometrically Distinct Paths (Figure 2)). Two distinct geodesic paths connecting the same start and target points, q_s and q_g , are called topo-geometrically distinct if there exists a common point, q , on the paths at which they have distinct path neighborhoods.

At this point we do not explicitly define or restrict the shape or size of the *path neighborhoods*. The effect of parameters determining the shape and size of these neighborhoods will be discussed later, and in general will constitute tunable parameters that determine the performance of the algorithm (in terms of thresholds on size and shape of obstacles or high-curvature/cost regions that give rise to multiple topo-geometric classes).

In practice, this allows us to run a wave-front propagation type algorithm, starting from q_s , and when different *branches* of the wave-front meet (around an obstacle and/or high-curvature/cost regions), allows us to keep track of the different branches and keep the branches separated by distinguishing between (and identifying them as distinct) copies of the same configuration point reached via distinct topo-geometric classes (Figure 3(a-d)). The two branches leading to the point q , and eventually to the goal, q_g , returns paths to those points in distinct topo-geometric classes (Figure 3(e-g)).

III. ALGORITHM DEVELOPMENT

A. Preliminaries: Graph Search-based Planning

1) *Discrete Graph Representation of a Configuration Space for Shortest Path Planning:* In traditional graph-search based shortest path-planning in a configuration space, a graph

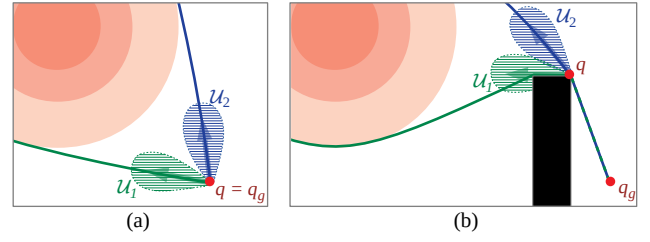


Fig. 2: Paths to a point q_g in the configuration space in distinct topo-geometric classes have distinct tangent vectors (arrows) at a point q (with $q = q_g$ in case (a), but a point other than q_g in case (b)). Instead of comparing and distinguishing the classes by their tangent vectors (which is often computationally difficult), a reasonable approach is to compare the *path neighborhoods* (shown by hatched/shaded regions) in the proximity of the paths near the point q .

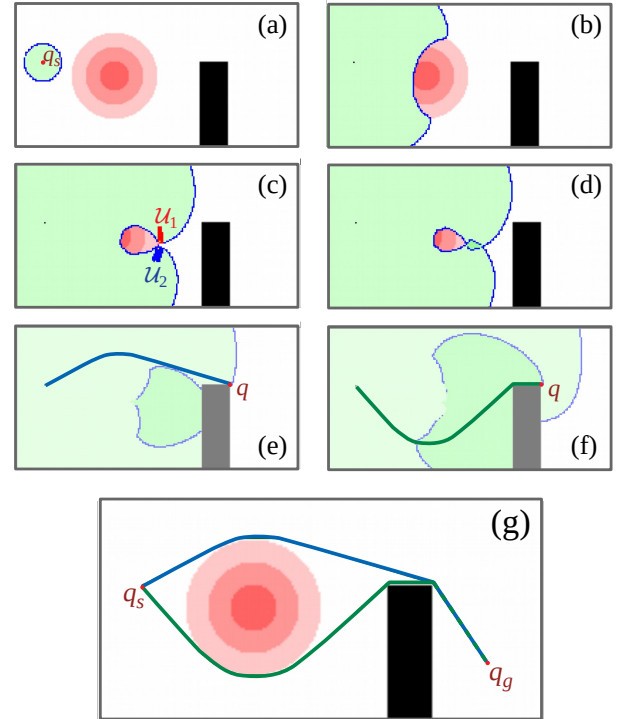


Fig. 3: Overview of the proposed *topo-geometric path planning* using search in *neighborhood-augmented graph*: (a-b) Search propagates as a uniform wave-front before encountering any obstacle or high-cost region. (b-c) Two branches of the search emerge as the search wave-front is disturbed by the increased costs. (c) When two branches meet, paths leading up to the same configuration point will have disjoint path neighborhood sets (\mathcal{U}_1 and \mathcal{U}_2). (d) Branches stay separate as a result. (e) To paths to q in distinct topo-geometric classes are found as (e) the first branch reaches the point q , (f) followed by the second branch. (g) Eventually the branches reach q_g and two paths in distinct topo-geometric classes are obtained.

$G = (V, E)$, is constructed as a discrete representation the configuration space, where the vertex set consist of points sampled (uniformly or in a randomized manner) from the valid configuration space. A vertex, $q \in V$, is typically represented by its spatial coordinates, and an edge $e = (q_1, q_2) \in E \subseteq V \times V$ connects neighboring vertices q_1 and q_2 . Search-based algorithms construct and explore the graph in an incremental manner: Starting at a start vertex, $q_s \in V$, it uses a wavefront propagation type approach, where it maintains an *open list* (the *exploration front*) and generates new neighboring vertices of the open list as it expands the *front*. This process continues until a desired goal vertex, $q_g \in V$, is reached. While there is a vast variety of search based algorithms – some purely for finding shortest paths in graphs (such as Dijkstra’s, A* [5, 6]), some using line-of-sight type information for finding paths that are closer to optimal in the underlying configuration space (Theta* [10]), and others construct simplicial complexes from the graph for achieving the same without line-of-sight information (such as S* [12]) – at their core they require a *neighbor or successor function*, \mathcal{N}_G , with the following properties:

- i. Given a vertex $q \in V$, $\mathcal{N}_G(q)$ returns the *neighbors* (vertices that are connected to q by edges) of the vertex (and the cost of the edges connecting them);
- ii. The algorithm also needs to be able to tell if a vertex returned by the neighbor function is something already explored/encountered in the past. For the usual discrete graph representation of a configuration space, this is usually as simple as comparing the coordinates of the new vertex with the coordinates of the existing/explored vertices.

On a graph that represents an obstacle-free Euclidean space, the search will propagate as a uniform wave. The exact shape of the search wave will depend on the specific search algorithm and the heuristic (if any being used). In case of planning in spaces with obstacles or nonuniform path costs these artifacts will obstruct or slow down the propagation of the search in certain directions as shown in Figure 4(a). As a result, multiple branches of the search wave will emerge, following through alternative paths around the artifact. However, when two branches meet at the downstream of the artifact (*downstream* of the artifact refers to the set of vertices that are further away from the start vertex compared to the artifact), they merge into one, as they pass through vertices with the same coordinates. Therefore, the traditional approach does not allow any distinction between paths, or even multiple paths to be found to the same vertex.

2) *Augmented Graph for Multi-class Path Planning*: In order to find multiple paths to the same vertex in the configuration space using a search-based approach, an *augmented graph*, $G_A = (V_A, E_A)$, needs to be constructed from G . Vertices in V_A are of the form (q, α) for $q \in V$ and α an invariant of a path class (*i.e.* a value/quantity – numeric or otherwise – that uniquely identifies the path class). Thus, corresponding to a vertex $q \in V$ there are multiple vertices

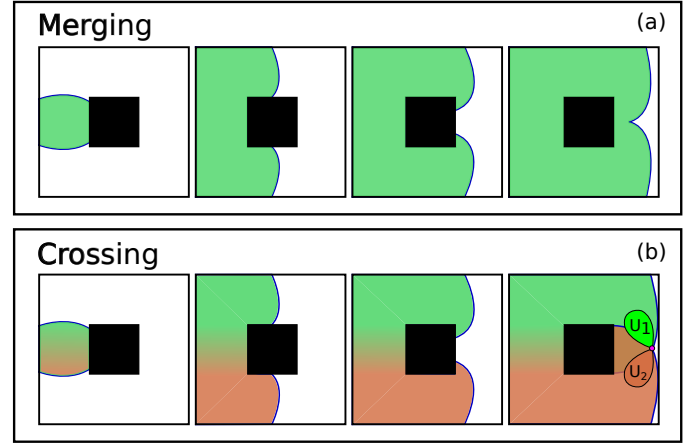


Fig. 4: Illustration of search progress in G vs. G_U : (a) Stages of search on a regular (non-augmented) discrete graph, G , representation of the configuration space demonstrates how different branches emerge and merge due to an obstacle in the environment. (b) Stages of search on a neighborhood-augmented graph demonstrates how different branches emerge and stay separated (different colors have been used to indicate different branches that remain separated). When a point, q , can be reached via different branches, corresponding path neighborhood sets (\mathcal{U}_1 and \mathcal{U}_2) are disjoint, and hence are represented by two distinct vertices, $(q, \mathcal{U}_1), (q, \mathcal{U}_2) \in V_U$. Two distinct paths to q are obtained by reconstructing path from (q, \mathcal{U}_1) and (q, \mathcal{U}_2) in G_U .

of the form $(q, \alpha_1), (q, \alpha_2), \dots \in V_A$, each corresponding to the vertex q reached via a different path class identified by invariants $\alpha_1, \alpha_2, \dots$.

An Example – h -augmented Graph: The idea is most easily demonstrated by the construction of h -augmented graph in context of topological path planning in multiple homotopy classes [14, 13, 15]. The idea behind construction of the h -augmented graph, $G_h = (V_h, E_h)$, is to append each vertex of G with the homotopy invariant of a path (called the h -signature, which is represented by a “word” constructed by concatenating the letters corresponding to rays emanating from obstacles that the path crosses – Figure 1b) leading up to that vertex from a given start vertex $q_s \in V$. With the h -signature associated with the start vertex being the empty word, “”, the construction of this graph can be made in an incremental manner and allows the algorithm to keep track of the homotopy class of the paths leading to a vertex during the execution of a search (Figure 5 inset). This, in effect, allows us to distinguish a vertex based on the homotopy class of the path taken to reach it from the start – two branches of the search front (open list) in two different homotopy classes leading to the same vertex q_g in V actually leads to two distinct vertices in V_h .

Shortcomings of Multi-class Planning using h -augmented Graph: One common challenge in computing topological invariants such as h -signature is that their computation requires geometric constructions based on a complete knowledge of ob-

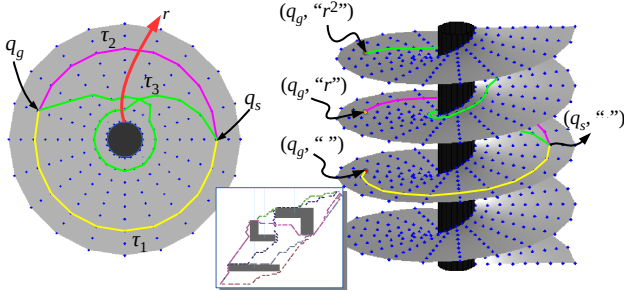


Fig. 5: Visualization of the h -augmented graph [14, 13, 15]: *Left*: A planar configuration space (light gray), with a single obstacle (black), and the vertex set, V (blue dots), in it. *Right*: The vertex set, V_h . Note how the trajectories *lift* to have different goal points of the form $(q_g, *) \in V_h$ corresponding to the same goal $q_g \in V$. *Inset*: Optimal paths in different homotopy classes in an environment with multiple obstacles.

stacles in the environment (rays in the 2-D case, for example – Figure 1b). For higher dimensional and complex configuration spaces, it becomes non-trivial to make analogous geometric constructions (Figure 1c), and even if such constructions are possible, the computation of h -signature needs to consider equivalence of certain set of words [24]. Furthermore, although topological path planning using h -augmented graph can efficiently compute multiple, locally optimal and topologically distinct paths, they are still unable to compute multiple paths within the same topological class that could be geometrically distinct. This scenario usually occurs when planning on a surface with non-zero curvature or in 3D spaces with genus-0 obstacles (Figure 1(d-f)).

B. Neighborhood Augmented Graph

In order to do away with complex geometric constructions in topological path planning, and to be able to find locally-optimal paths in distinct topo-geometric classes (Definition 3), in this paper we proposed a *neighborhood-augmented graph*, $G_{\mathcal{U}} = (V_{\mathcal{U}}, E_{\mathcal{U}})$, that is constructed from the given discrete graph representation of the underlying configuration space, $G = (V, E)$, by augmenting each vertex with a “*path neighborhood*” that is representative of the tangent vector of the path leading to the vertex (Figure 2). Just like the previously-described augmented graphs, corresponding to a vertex $q \in V$, there can exist multiple distinct vertices, $(q, \mathcal{U}_1), (q, \mathcal{U}_2), \dots \in V_{\mathcal{U}}$, where each \mathcal{U}_i consist of **references/pointers to vertices in $V_{\mathcal{U}}$** (i.e., $\mathcal{U}_i \subset V_{\mathcal{U}}$) that make up the neighborhood of a portion of the path leading the vertex (q, \mathcal{U}_i) . We refer to each such \mathcal{U}_i as a *path neighborhood set* corresponding to the path leading to the vertex v .

For topo-geometrically distinct paths, the path neighborhood sets are expected to be disjoint as illustrated in Figures 4(b) & 2. While, if a vertex is reached from the same topo-geometric class (e.g., from a different parent/vertex), there

will be significant overlap between the path neighborhood sets. Thus, we define

Definition 4 (Equivalence of Vertices in $G_{\mathcal{U}}$). *Given $(q, \mathcal{U}), (q', \mathcal{U}') \in V_{\mathcal{U}}$, they are called equivalent (i.e., considered to be the same vertex, and denoted as $(q, \mathcal{U}) \equiv (q', \mathcal{U}')$, if $q = q'$ and $\mathcal{U} \cap \mathcal{U}' \neq \emptyset$.*

This comparison of vertices is critical in incremental construction of the graph, $G_{\mathcal{U}}$ – every time a new vertex is generated, it can be compared against already-generated/existing vertices to determine if it is a new vertex or if it is the same vertex as an existing one.

An Implementational Detail: It is to be noted that for two path neighborhood sets to intersect (i.e., for the computation of $\mathcal{U} \cap \mathcal{U}'$), they must contain a common vertex that not only has the same coordinates/configuration but also the same path neighborhood sets (that is, $\mathcal{U} \cap \mathcal{U}' \neq \emptyset \iff \exists (w, \mathcal{W}) \in \mathcal{U}, (w', \mathcal{W}') \in \mathcal{U}'$ s.t. $(w, \mathcal{W}) \equiv (w', \mathcal{W}')$). At a first glance it may appear that the computation of equivalence thus requires an iterative computation of other equivalences for vertices in the path neighborhood sets. However, in implementation, since path neighborhood sets are stored as *pointers* to vertices in $V_{\mathcal{U}}$, it is sufficient to check if the sets of pointers, \mathcal{U} and \mathcal{U}' , have any common pointer. If the pointers are the same, that will automatically imply that they have the same (hence overlapping) path neighborhood sets (since otherwise they would have been identified as different vertices in the first place and would have been assigned different pointers).

Neighbor/Successor Function: For any vertex $(q, \mathcal{U}) \in V_{\mathcal{U}}$, the neighbor function of the configuration graph, G , returns the configuration of (which are usually represented by coordinates in the configuration space) vertices that are adjacent to q . Suppose $\{q_1, q_2, \dots\} = \mathcal{N}_G(q)$. The path neighborhood sets of each q_i is then computed by actually computing a neighborhood (by collecting pointers to vertices in $V_{\mathcal{U}}$) of (q, \mathcal{U}) by performing a short secondary exploration/search in the current/existing $G_{\mathcal{U}}$. The details of this secondary search is described in Section III-C. If this secondary search returns a path neighborhood set \mathcal{U}' , the neighbor/successor function of $G_{\mathcal{U}}$ can then be described as $\{(q_1, \mathcal{U}'), (q_2, \mathcal{U}'), \dots\} = \mathcal{N}_{G_{\mathcal{U}}}((q, \mathcal{U}))$. The cost of each edge on $G_{\mathcal{U}}$ is the same as its projection on the original graph G (that is, $\mathcal{C}_{G_{\mathcal{U}}}((q, \mathcal{U}), (q_i, \mathcal{U}')) = \mathcal{C}_G(q, q_i)$).

A search in the graph $G_{\mathcal{U}}$ can be performed using any search algorithm. Throughout this paper we have presented results from searches in $G_{\mathcal{U}}$ performed using Dijkstra’s search, using A* searches (with appropriate heuristic function), and with S* search [12] for computing different topo-geometrically distinct paths that are optimal in the underlying configuration space.

As a simple illustration, however, we present a pseudo-code for the search using Dijkstra’s algorithm on an incrementally constructed neighborhood-augmented graph in Algorithm 1. The traditional way to use this algorithm is to insert the goal-based stopping criteria given in Algorithm 2 as the input, provided a goal coordinate and number of desired paths. However, depending on the application, there could be other

Algorithm 1 Incremental Construction and Dijkstra's Search in a Neighborhood-augmented Graph (NAG)

 $G_{\mathcal{U}} = \text{searchNAG}(q_s, \mathcal{N}_G, \mathcal{C}_G, @\text{stopSearch})$

Inputs:

- a. Start configuration $q_s \in V$
- b. Neighbor/successor function \mathcal{N}_G (this describes the connectivity of graph G)
- c. Cost function $\mathcal{C}_G : V \times V \rightarrow \mathbb{R}_+$
- d. Stopping criteria (function), $\text{stopSearch} : V_{\mathcal{U}} \rightarrow \{0, 1\}$

Output:

Graph $G_{\mathcal{U}}$, with costs and neighborhoods computed for every vertex

```

1:  $v_s := (q_s, \{\&v_s\})$  // start vertex in  $V_{\mathcal{U}}$ , with self-reference
   // in its path neighborhood set.
2: Set  $g(v_s) = 0$  // g-score
3:  $V_{\mathcal{U}} = \{v_s\}$  // vertex set
4:  $E_{\mathcal{U}} = \emptyset$  // edge set, maintained implicitly as a link tree/graph
5:  $Q = \{v_s\}$  // open list, maintained by a heap data structure.
6:  $v := v_s$ 
7: while  $Q \neq \emptyset$  AND not  $\text{stopSearch}(v)$  do
8:    $v := (q, \mathcal{U}) = \text{argmin}_{v' \in Q} g(v')$  // heap pop.
9:    $Q = Q - v$  // heap pop.
10:   $\mathcal{U}' = \text{computePNS}(v, G_{\mathcal{U}})$  // path neighborhood set
   // for path leading to  $v$ 
11:  for  $q' \in \mathcal{N}_G(v)$  do
12:     $v' := (q', \mathcal{U}')$  // potential neighbor/successor
13:     $g' = g(v) + \mathcal{C}_G(q, q')$  // potential g-score for  $v'$ 
14:    if  $\nexists w \in V_{\mathcal{U}}$ , with  $v' \equiv w$  then // new vertex
15:       $V_{\mathcal{U}} = V_{\mathcal{U}} \cup \{v'\}$ 
16:       $E_{\mathcal{U}} = E_{\mathcal{U}} \cup \{(v, v')\}$  // maintained as linktree
   // for neighbor function computation,  $\mathcal{N}_{G_{\mathcal{U}}}$ 
17:       $g(v') = g'$ 
18:       $Q = Q \cup \{v'\}$ 
19:       $v'.\text{came\_from} = v$ 
20:    else // vertex already exists ( $w$ )
21:       $E_{\mathcal{U}} = E_{\mathcal{U}} \cup \{(v, w)\}$ 
22:       $w = \text{updatePNS}(w, v')$ 
23:      if  $g' < g(w)$  AND  $w \in Q$  then // update  $w$ 
24:         $g(w) = g'$ 
25:         $w.\text{came\_from} = v$ 
26:   $G_{\mathcal{U}} := (V_{\mathcal{U}}, E_{\mathcal{U}})$ 
27: return  $G_{\mathcal{U}}$ 

```

Algorithm 2 Goal-Based Stopping Criteria for Search

 $[\text{bool}, \mathcal{V}_g] = \text{stopSearch_AtGoal}_{q_g, n_p}(v)$

Input: Current vertex $v = (q, \mathcal{U}) \in V_{\mathcal{U}}$

Static variables / parameters:

- a. Goal configuration $q_g \in V$
- b. Number of paths to find n_p

Output:

- a. Boolean (**true** to stop search, **false** to continue)
 - b. Vertices in the NAG found at goal configuration \mathcal{V}_g
-

```

1: static  $\mathcal{V}_g (= \emptyset)$  // static variable initiated with empty set
2: if  $v.q = q_g$  AND  $v \notin \mathcal{V}_g$  then
3:    $\mathcal{V}_g = \mathcal{V}_g \cup v$ 
4:   return  $(|\mathcal{V}_g| == n_p)$ 

```

uses of the algorithm, utilizing alternative stopping criteria, as it will be further discussed in Section V-B.

Figure 6 illustrates the incremental construction of a neighborhood-augmented graph based on a given discrete graph. Two separate search *branches* emerge due to a hole in the underlying discrete graph. Neighborhoods for selected vertices are shown in the bottom row. Vertices shown in the first three columns are trivially distinct as they do not share the same coordinates. In the fourth column, two vertices with the same coordinates (*i.e.*, the same vertex in G) are selected for which the path neighborhood sets are disjoint as they are reached via different branches of the search. As a result, two copies of vertices (with two disjoint path neighborhood sets) are maintained separately within the neighborhood-augmented graph. Whenever a distinct vertex at the goal coordinates is expanded, it is possible to reconstruct a topo-geometrically distinct path from the start to the goal coordinate using the corresponding goal vertex and the constructed neighborhood-augmented graph with a *path reconstruction* subroutine. Two of such paths are shown in the last column of Figure 6.

For given shape characteristics/geometry of the path neighborhood sets, and geometric artifacts of the configuration graph (influenced by holes, obstacles, high-cost or non-zero curvature regions), branches of the search around such artifacts may not merge, but stay separate (cross-over) and progress further, as there can be vertices at the same coordinates that are reached via significantly different paths and hence have different path neighborhood sets. The effect of the size/geometry of the path neighborhood sets on the ability to find multiple topo-geometric classes around obstacles of different size/geometry is discussed in more detail in Section III-D. Performing the search on the neighborhood-augmented graph computes alternative and locally optimal paths that are topo-geometrically different than the globally optimal path. An illustration of the path search using S* search algorithm in a discrete representation of a continuous configuration space using a neighborhood-augmented graph is shown in Figure 4(b).

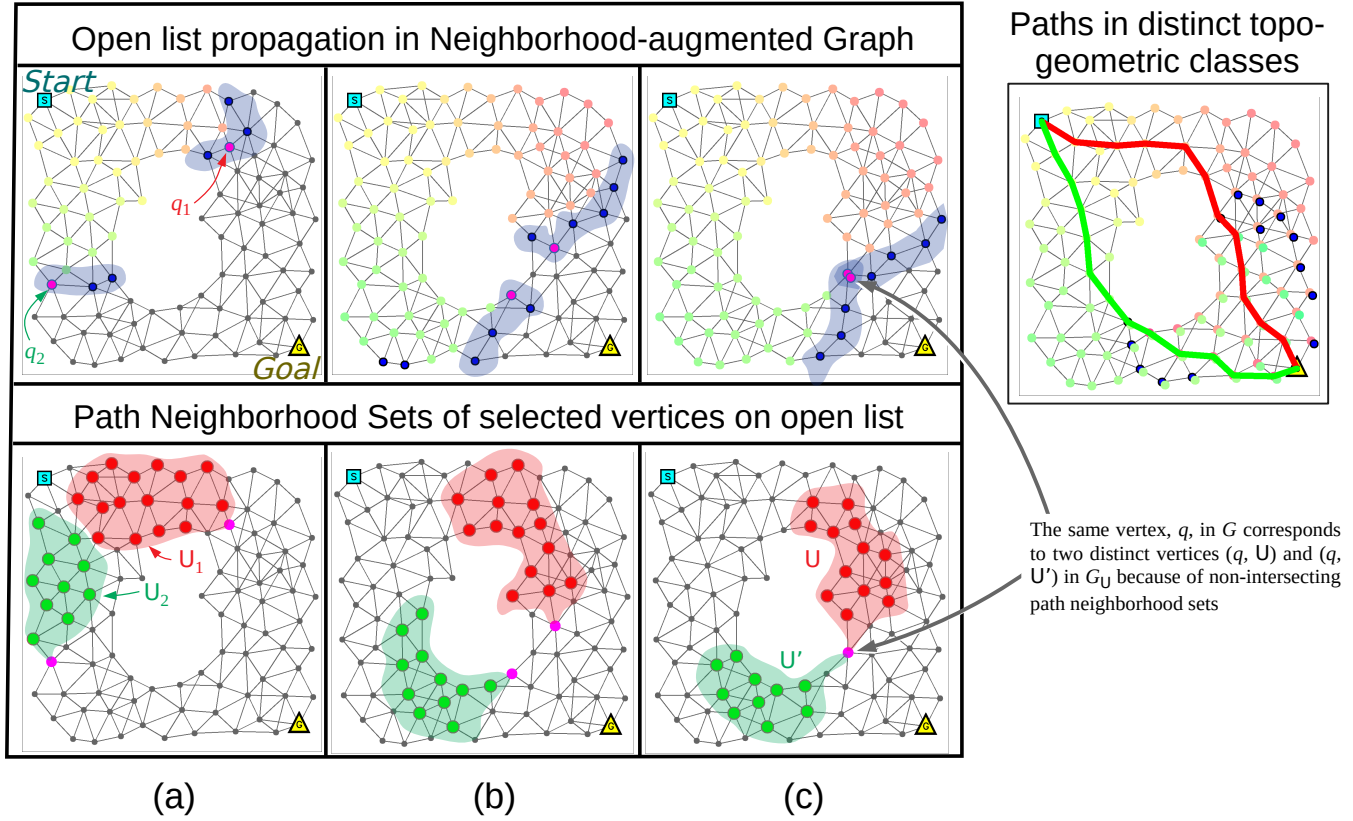


Fig. 6: Path planning on neighborhood-augmented graph, G_U , using Dijkstra’s search (actual result, with highlights and labeling for aiding explanation). The planar graph that is visible in the figures is the configuration graph $G = (V, E)$. The neighborhood-augmented graph is constructed incrementally, and the top row shows the vertices in the *open list* at different instants during progress of the search (colored/highlighted in blue). However, a vertex in the neighborhood-augmented graph, G_U , is not just a vertex in G , but also contains information about a path neighborhood set leading to the vertex (maintained as a list of pointers to already-generated vertices in V_U). This is shown in the second row, where two vertices, (q_1, \mathcal{U}_1) and (q_2, \mathcal{U}_2) , in the two different *branches* of the search (created due to the central *hole*) in the graph, are chosen to illustrate their respective path neighborhood sets (shown/highlighted in red and green respectively). However, as demonstrated in column (c) of the figure, when the two branches *meet*, corresponding to the same vertex q in the configuration graph, we end up constructing two distinct vertices, (q, \mathcal{U}) and (q, \mathcal{U}') , in G_U . Two locally shortest paths in distinct topo-geometric classes to the goal are found as a result (last column). The cost function use for the search is the Euclidean distance between the vertices.

C. Neighborhood Generation

During the search in the neighborhood-augmented graph (Algorithm 1 – also referred to as **primary search** henceforth), a path neighborhood set, \mathcal{U} , of a vertex $v \in V_U$ need to be computed (this consists of a set of vertices within some distance r of v in the neighborhood of the path leading to v in the neighborhood-augmented graph) – Line 10 of Algorithm 1. To compute this path neighborhood set, a *secondary search* is performed on the current neighborhood-augmented graph, G_U (using A* algorithm), starting from the vertex of interest v . We emphasize that this secondary search (which will be referred to as **neighborhood search** from now on) occurs on the existing graph, G_U , during which G_U remains unchanged.

If the neighborhood search is carried out until a distance r from v (reaching a g -score of r), the expanded vertices will

form a shape similar to a half-disk around v , bounded by a circle of radius r at the upstream and by the open list of the primary search at the downstream (Figure 7(a)). However, a disk-shaped set does not provide a reasonable representation for a neighborhood around the path leading up to v . It is possible to modify the shape of the computed path neighborhood set by utilizing the existing g -score of vertices from the primary search. By using the g -score from the primary search as heuristic function to guide the secondary search (Line 16 of Algorithm 3), we obtain a path neighborhood set that *hugs* the path more closely.

A pseudo-code for the neighborhood search (*computePNS* routine) is provided in Algorithm 3. Figure 7a,b are visualizations of the search progress with a disc-shaped neighborhood and a path neighborhood.

Algorithm 3 Path Neighborhood Set (PNS) Computation using A* Search

$$\mathcal{U} = \text{computePNS}_{\{r, \omega, \text{neighborhood_conic}\}}(v_p, G_{\mathcal{U}})$$

Inputs:

- a. Existing/current neighborhood-augmented graph $G_{\mathcal{U}} = (V_{\mathcal{U}}, E_{\mathcal{U}})$, along with the g-scores of vertices in the graph, $g(\cdot)$.
- b. Parent vertex $v_p = (q_p, \mathcal{U}_p) \in V_{\mathcal{U}}$

Geometry Parameters:

- a. Neighborhood radius, $r \in \mathbb{R}_+$
- b. Heuristic weight, $\omega \in [0, 1]$
- c. Rollback amount, $r_b \in \mathbb{Z}_{\geq 0}$

Output:

A set of vertices (*path neighborhood set*), $\mathcal{U} \subset V_{\mathcal{U}}$

```

1:  $v_s := \text{rollback}(v_p, r_b)$  // start vertex for secondary search
2:  $\mathcal{U} := \emptyset$ 
3:  $\tilde{g}(v) = \infty, \tilde{f}(v) = \infty, \forall v \in V_{\mathcal{U}}$  // implicitly set all f- and g- score for secondary search to infinity for all vertices
4:  $\tilde{g}(v_s) := 0$  // g-score in secondary search
5:  $\tilde{f}(v_s) := \tilde{g}(v_s) + \omega g(v_s)$ , // f-score in secondary search. g refers to the g-score from the primary search, which is being used as a heuristic function for the secondary search
6:  $\mathcal{U} = \{v_s\}$  // vertex set for neighborhood search
7:  $\tilde{Q} := \{v_s\}$  // open list for neighborhood search
8:  $v := v_s$ 
9: while  $\tilde{Q} \neq \emptyset$  AND not  $\tilde{g}(v) > r$  do
10:    $v := \text{argmin}_{v' \in \tilde{Q}} \tilde{f}(v')$ 
11:    $\tilde{Q} = \tilde{Q} - v$ 
12:   for  $v' \in \mathcal{N}_{G_{\mathcal{U}}}(v)$  do
13:      $\bar{g}' = \tilde{g}(v) + \mathcal{C}_{G_{\mathcal{U}}}(v, v')$ 
14:     if  $\bar{g}' < \tilde{g}(v')$  then // better g-score
15:        $\tilde{g}(v') = \bar{g}'$ 
16:        $\tilde{f}(v') = \bar{g}' + \omega g(v')$ 
17:        $\tilde{Q} = \tilde{Q} \cup \{v'\}$ 
18:    $\mathcal{U} = \mathcal{U} \cup \{v'\}$ 
19: return  $\mathcal{U}$ 

```

A path neighborhood set of a vertex needs to satisfy following conditions to achieve desired branching behavior around the artifacts of the search space:

- 1) Vertices at the same coordinates generated through parent vertices that are close to each other in the graph should have large overlap in path neighborhood set. Essentially, a branch of the search should not be giving rise to any subbranches unless it encounters an obstacle or a high-cost region. Size of the path neighborhood sets of nearby vertices in the same branch of a search should be large enough to contain common vertices.
- 2) For an obstacle or a high-cost region to generate multiple topo-geometric classes/branches during the search, the size of path neighborhood set should be smaller than

the size of the obstacle/high-cost region to ensure that there will not be any intersection at the upstream of the artifact (Figure 7, second row). Hence, vertices generated via parent vertices on a different branch will be identified as different.

The effect of the size of path neighborhood sets relative to the obstacle size can be observed in Figure 7c,d. As observed empirically, disk-shaped path neighborhood sets are more sensitive to the size parameter than the *path-hugging* path neighborhood sets as they tend to overlap at the upstream of an artifact even for smaller radii. Therefore, *path-hugging* path neighborhood sets are to be considered as the default path neighborhood sets shape unless stated otherwise.

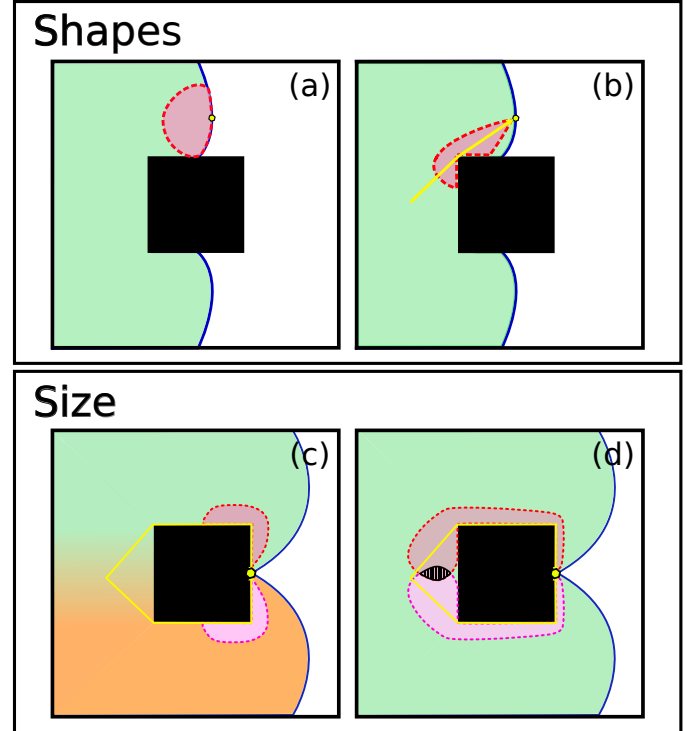


Fig. 7: (a) Disk-shaped neighborhood at a vertex of interest (VOI). (b) *Path-hugging* neighborhood at a VOI (Default option for path neighborhood sets). (c) Disjoint neighborhoods for two vertices at the same coordinates due to the obstacle resulting in the second copy to be inserted to the neighborhood augmented graph. (d) Intersecting neighborhoods at the upstream of the same obstacle, when the neighborhood size is increased. The second vertex is equivalent to the first one, thus it will be discarded.

D. Implementation Details

The main ideas and procedures of the search on a neighborhood augmented graph is as described in previous sections. However, there are certain details and modifications in terms of the implementation of these ideas that are worth mentioning.

Rollback to grandparent. In previous sections, it is assumed that the neighborhood search for a vertex v' starts

from its parent vertex v . As a result, path neighborhood sets are always illustrated as attached to the vertex. However, depending on the primary search algorithm being used, at the time of neighborhood search, vertex v might not be inserted in the neighborhood-augmented graph, thus making it impossible to perform a search starting from v (this mainly occurs when using S^* , as the algorithm generates the grandchildren when expanding a vertex). A solution is to *rollback* from the vertex v' for some fixed number of generations (which means to consider the parent or n -th grandparent of the vertex) and start the neighborhood search from that vertex. This procedure is performed by the *rollback* subroutine in Line 1 of Algorithm 3, which recursively calls the ‘came_from’ attribute of a vertex for desired number of times.

Neighborhood merging. Whenever two vertices are identified as equivalent during the primary search ($w \equiv v'$), it is an option to get the union of their path neighborhood sets and assign it to the vertex that is going to be kept in the graph ($w.\mathcal{U} := w.\mathcal{U} \cup v'.\mathcal{U}$). This option is referred to as *neighborhood merging*. *Neighborhood merging* essentially eliminates the randomness in the neighborhoods that might arise due to the randomness in the order of vertex expansions. This is implemented in the *updatePNS* subroutine in Line 22 of Algorithm 1.

Threshold for neighborhood comparison. Around the start vertex of the primary search, paths are short, thus some path neighborhoods that are supposed to be intersecting might remain disjoint (especially when paths are pointing in opposite directions). This might cause some spurious topo-geometric classes to be generated around the start. A solution is to have a threshold radius around the start, within which the neighborhood comparison is not triggered.

Generation number. In previous sections, neighborhood radius r was expressed in terms of the g-scores on the corresponding graph. However, neighborhood radius is implemented as generation numbers (in other words the search depth). Generation number refers to the generations in between two vertices (i.e. for the immediate parents of a vertex, generation number is 1, for grandparents its 2).

E. Results

Path-planning using the neighborhood augmented graph can identify distinct paths in a 2D environment with obstacles, high-cost regions, or a mixture of both. In a 3D environment, it can identify distinct path in the presence of objects with non-zero genus, or even more complex structures such as knots and chains. Examples for 2D and 3D scenarios are provided in Figure 8(a)-(f).

Cost Multiplier Analysis: As usual on uniform cost and flat (zero curvature) environments (Figure 8a), the path cost between two vertices is computed using the Euclidean distance as $c(v_i, v_j) = d(v_i, v_j)$, where $d(v_i, v_j) = \|v_i - v_j\|_2$. For environments with high-cost regions (as in Figure 8b,c), the path cost between two vertices is implemented as a function of the color of the corresponding cells and a cost multiplier (CM). Let $\rho(v) : V \rightarrow [0, 1]$ map the given vertex to the

color value. Then the path cost between two vertices in a nonuniform path cost environment is computed as $c(v_i, v_j) = (v_i, v_j) \left[1 + \text{CM} \frac{\rho(v_i) + \rho(v_j)}{2} \right]$.

Shortest paths obtained by the neighborhood augmented planning method varies with the cost multiplier being used in the environment. Figure 9 shows how locally shortest paths tend to get closer to the center of the high cost region as the cost multiplier decreases. It is worth noting that above a certain value of the cost multiplier paths will not move further away from the high cost region. At the other extreme (if the cost multiplier is below a certain value), proposed algorithm will become incapable of distinguishing between multiple shortest paths and return only one of them (see the path for $\text{CM} = 1$ in Figure 9). This issue is explained further in detail and tackled in Section IV.

IV. MODIFIED ALGORITHM FOR LOW CURVATURE/COST ENVIRONMENTS

A. Limitations

As explained in Section III-B, comparison of neighborhoods allow distinction between vertices with the same coordinates that are reached via different branches of the search. However, the branching of the search is only possible in the presence of obstacles and high-cost regions in 2D and obstacles with genus-1 or higher in 3D. As the curvature of an environment (slope/height of a hill, path costs at the high-cost region or cost multiplier) decreases, the search propagation through that region is not slowed down enough to give rise to two clear branches. Instead, only a small cusp in the search wave is generated. Similarly, around a corner of a prism in 3D, the search is only slowed down by a small amount through the corner. When the branches are not generated naturally, the neighborhoods maintain an overlap even around high-cost regions and prismatic obstacles in 3D, thus keeping the search propagating as a uniform wave after encountering the artifact. This behavior is shown in Figure 10(b),(c). In these cases, only a single path is available as a result of the search on the neighborhood augmented graph.

B. Merge Points

As one can imagine, the transition from a low curvature environment (limiting scenario) to a high curvature environment (working scenario) is a continuous spectrum. In other words, it is possible to start with an entirely flat surface without any obstacles and introduce an infinitesimal curvature (bump) that would grow infinitesimally to achieve a hill with desired slope/height. On a flat surface without any obstacles, there is a unique shortest path between any two points, and it is neither expected nor necessary to achieve a branching in the search wave. However, as demonstrated, the branching behavior is desirable for some curvature that is significantly large. Although it cannot be guaranteed that the proposed approach (neighborhood augmented graph search) will deal with any type of curvature in this spectrum, some modifications can be introduced to increase the capabilities of

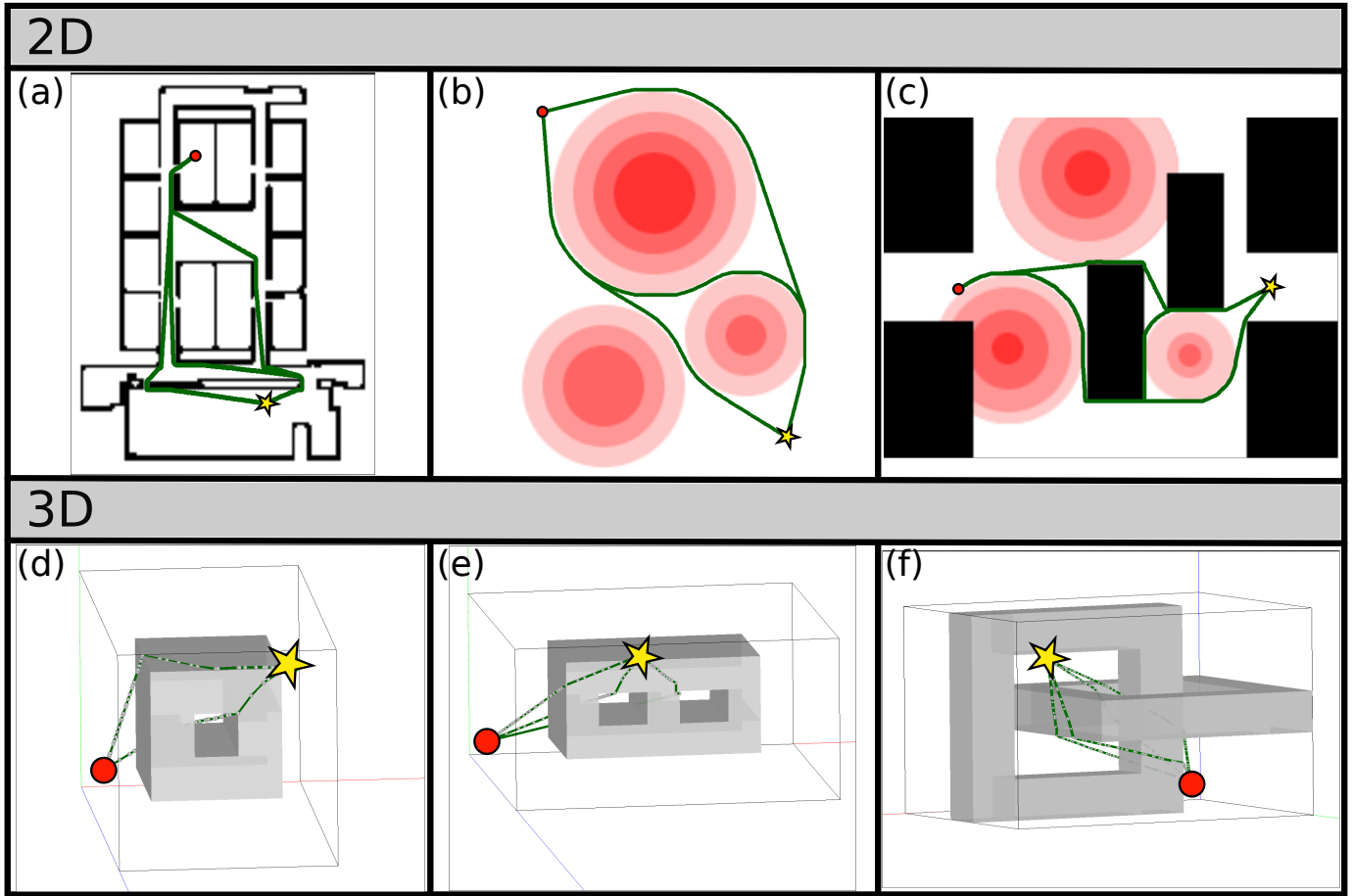


Fig. 8: **Results:** (a) Distinct paths found in a 2D building-like environment (3 paths). (b) Environment with multiple hills (high-cost centers) (3 paths). (c) Environment with a mixture of obstacles and hills (3 paths). (d) 3D environment with genus-1 object (2 paths). (e) 3D environment with genus-2 object (3 paths). (f) 3D environment with a chain-like structure (4 paths).

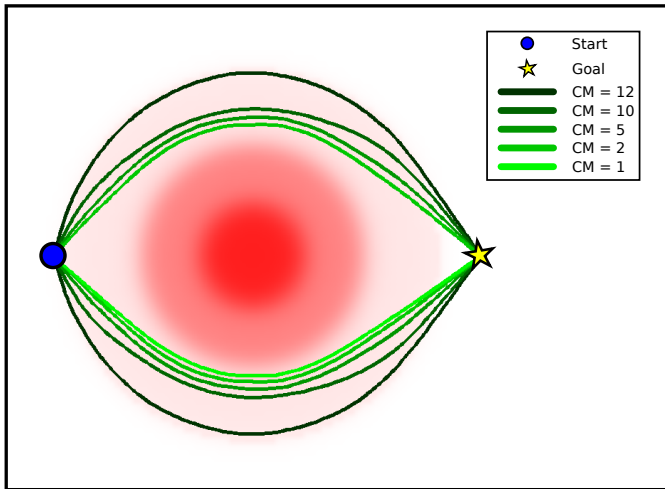


Fig. 9: **Results:** Shortest paths obtained on a nonuniform cost environment. As cost multipliers (CM) decrease, shortest paths tend to get closer to the high cost region. For $CM = 1$, the algorithm can only find a single path.

the approach on low curvature environments. One can draw analogies between the nonuniform path cost scenarios and the genus-0 prism scenarios in 3D, by interchanging the references to the slope of a hill with the curvature at a 3D corner.

As described in previous sections, two vertices are equivalent on a neighborhood augmented graph if they have identical coordinates and intersecting neighborhoods. However, it is an option to use an intersection threshold (ϵ_{ni}) (as a ratio of the number common elements of the tangent neighborhood sets to the size of the path neighborhood sets), below which the intersection is not considered as significant and the vertices are considered as inequivalent.

By reducing the neighborhood radius and introducing a neighborhood intersection threshold, it is possible to turn some pairs of vertices that would normally be identified as equivalent into distinct vertices. When implemented on the limiting scenarios (small hill, genus-0 prism in 3D), this method disturbs the uniform search wave that would normally be observed. However, this disturbance itself is not enough for separate branches to emerge (additional vertices generated on top of the existing ones are not distributed regularly to form a branch).

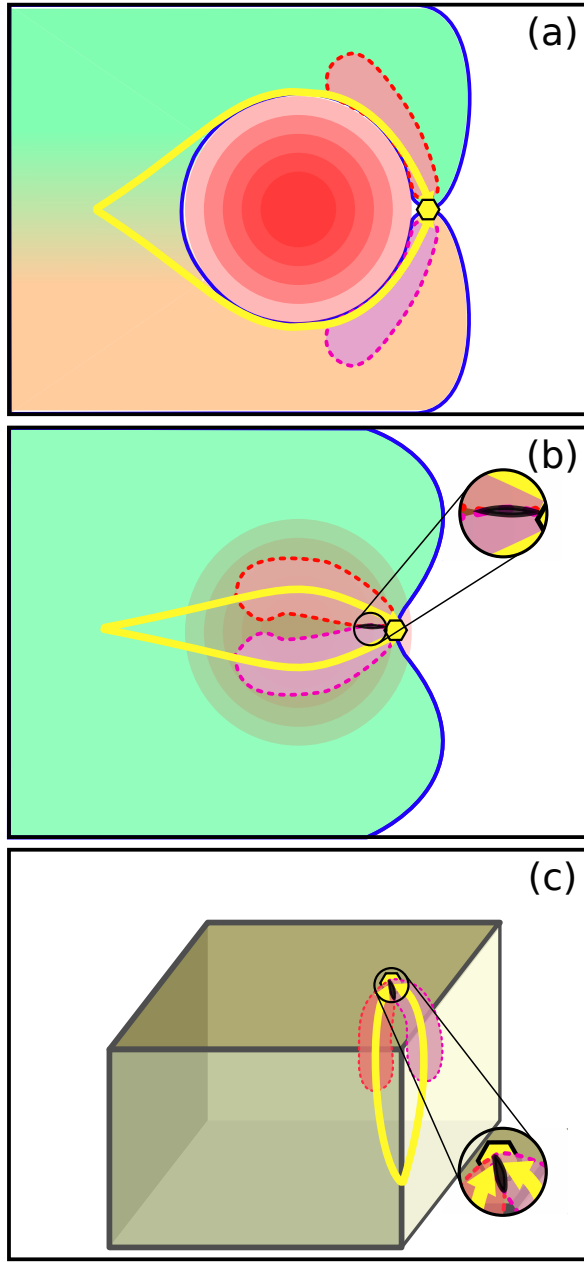


Fig. 10: (a) Through a steep hill (high-cost center with high value) search propagation is significantly slowed down, thus two branches emerge. Neighborhoods remain separate for vertices reached via different branches. (b) Around a flatter hill, (high-cost center with smaller value) neighborhoods maintain an overlap, hence branches do not emerge naturally even on a neighborhood augmented graph (Neighborhoods maintain the overlap, because the flatter hill only slows down the search through its center by a small amount, causing a small cusp in the search wave). (c) Same/similar behavior is observed around a corner of a 3D prism.

To regulate the branching behavior on such environments, an artificial cut in the search space is introduced. Abstractly, this artificial cut in the environment does not allow any

valid path to pass through, behaving almost like an obstacle. Implementation-wise, a set of vertices in the graph are identified as merge points through which the graph search is not allowed to propagate. A pair of vertices $v_i = (q_i, \mathcal{U}_i)$ and $v_j = (q_j, \mathcal{U}_j)$ are identified as merge points if they satisfy the following conditions:

- 1) v_i and v_j have identical coordinates, $q_i = q_j$
- 2) v_i and v_j have a neighborhood intersection that is below the set threshold, $|\mathcal{U}_i \cap \mathcal{U}_j| < \epsilon_{ni}$
- 3) The distance between v_i and v_j in the graph is less than some threshold ϵ_{mp}

Essentially, conditions 1 and 2 imply that $v_i \neq v_j$, hence both vertices are already distinct elements in $V_{\mathcal{U}}$. As $G_{\mathcal{U}}$ is a connected graph, there exists a path between v_i and v_j . Although v_i and v_j have identical coordinates, the length of this path is nonzero and is equal to the sum of the distances to their closest common neighbor from v_i and v_j . An illustration of the path between two merge points is given in Figure 11(a). A pseudo-code for the search on a neighborhood augmented graph with merge points is provided in Algorithm 4.

Merge points are identified within some region in the environment at the downstream of the high-cost center. A representative illustration of how this region gives rise to branches in the search is provided in Figure 11(b).

Path-planning using the neighborhood augmented graph with modified parameters and the addition of merge points can identify distinct paths in 2D environments with smaller bumps. In a 3D environment, it can identify distinct path around a corner of a prismatic obstacle. Examples for 2D and 3D scenarios are provided in Figure 12(a)-(d). In both 2D and 3D cases, a high cost center or a prismatic corner gives rise to two shortest paths, when the start and goal are placed symmetrically with respect to the artifact. However, when placed asymmetrically, the second path can only be identified with the help of the merge points (the artificial cut). Those paths that contain any merge points are considered as invalid as they are cornering around an artificial structure in the environment.

V. LENGTH CONSTRAINED SEARCH

A. Problem Description

Tethered robots are mostly deployed to perform tasks in environments where wireless communication is limited and/or robot is unable to operate without an external power source. This work is mainly interested in applications where a tethered robot is to navigate in a 3D environment with non-zero genus obstacles (refer to Figure 13 for examples of such environments). Examples include a drone tethered to an outside base navigating in and around a building with windows or gates or a disaster site with multiple entries and exits, an underwater robot tethered to the surface station navigating in and around a ship wreck or an underwater cave with tunnels and passages. In the context of path planning, the aim is to find a path between a start and a goal configuration in the configuration space of the tethered robot, that will satisfy the physical constraints brought by the tether.

Algorithm 4 Incremental Construction and Dijkstra's Search in a Neighborhood-augmented Graph (NAG) with Merge Points

$G_{\mathcal{U}} = \text{searchNAG_MP}(q_s, \mathcal{N}_G, \mathcal{C}_G, @\text{stopSearch})$

Inputs:

- a. Start configuration $q_s \in V$
- b. Neighbor/successor function \mathcal{N}_G (this describes the connectivity of graph G)
- c. Cost function $\mathcal{C}_G : V \times V \rightarrow \mathbb{R}_+$
- d. Stopping criteria (function), $\text{stopSearch} : V_{\mathcal{U}} \rightarrow \{0, 1\}$

Output:

Graph $G_{\mathcal{U}}$, with costs and neighborhoods computed for every vertex

```

1:  $v_s := (q_s, \{\&v_s\})$  // start vertex in  $V_{\mathcal{U}}$ , with self-reference
   // in its tangent neighborhood set.
2: Set  $g(v_s) = 0$  // g-score
3:  $V_{\mathcal{U}} = \{v_s\}$  // vertex set
4:  $E_{\mathcal{U}} = \emptyset$  // edge set, maintained implicitly as a link tree/graph
5:  $Q = \{v_s\}$  // open list, maintained by a heap data structure.
6:  $v := v_s$ 
7: while  $Q \neq \emptyset$  AND not  $\text{stopSearch}(v)$  do
8:    $v := (q, \mathcal{U}) = \text{argmin}_{v' \in Q} g(v')$  // heap pop.
9:    $Q = Q - v$  // heap pop.
10:  if  $v.\text{is\_merge\_point}$  then
11:    continue
12:   $\mathcal{U}' = \text{computeTNS}(v, G_{\mathcal{U}})$  // tangent neighborhood set
   // for path leading to  $v$ 
13:  for  $q' \in \mathcal{N}_G(v)$  do
14:     $v' := (q', \mathcal{U}')$  // potential neighbor/successor
15:     $g' = g(v) + \mathcal{C}_G(q, q')$  // potential g-score for  $v'$ 
16:    if  $\exists w \in V_{\mathcal{U}}$ , with  $v' \neq w$  AND  $q' = w.q$  then
   // new vertex at the same coordinates
17:      if  $\text{distanceInGraph}(v', w) < \epsilon_{mp}$  then
18:         $v'.\text{is\_merge\_point} = \text{True}$ 
19:         $w.\text{is\_merge\_point} = \text{True}$ 
20:      if  $\nexists w \in V_{\mathcal{U}}$ , with  $v' \equiv w$  then // new vertex
21:         $V_{\mathcal{U}} = V_{\mathcal{U}} \cup \{v'\}$ 
22:         $E_{\mathcal{U}} = E_{\mathcal{U}} \cup \{(v, v')\}$  // maintained as linktree
   // for neighbor function computation,  $\mathcal{N}_{G_{\mathcal{U}}}$ 
23:         $g(v') = g'$ 
24:         $Q = Q \cup \{v'\}$ 
25:         $v'.\text{came\_from} = v$ 
26:      else // vertex already exists ( $w$ )
27:         $E_{\mathcal{U}} = E_{\mathcal{U}} \cup \{(v, w)\}$ 
28:        if  $g' < g(w)$  AND  $w \in Q$  then // update  $w$ 
29:           $g(w) = g'$ 
30:           $w.\text{came\_from} = v$ 
31:           $w = \text{updateTNS}(w, v')$ 
32:   $G_{\mathcal{U}} := (V_{\mathcal{U}}, E_{\mathcal{U}})$ 
33: return  $G_{\mathcal{U}}$ 

```

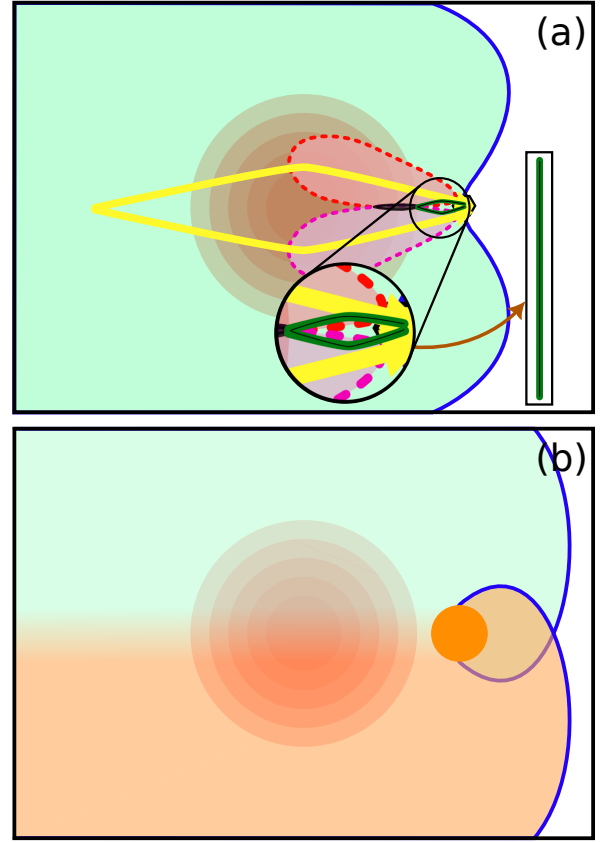


Fig. 11: (a) Visualization of the distance in the graph between two vertices with some overlap in neighborhoods. Such vertices that have small enough distance in the graph are detected as merge points. (b) On a low curvature environment, merge points are detected at the downstream of the hill. Treatment of these merge points causes branches to emerge around this region.

For the purposes of this paper, it can be assumed that the tether is made from an elastic material with a maximum length l , which remains taut during the entire operation irrespective of the location of the robot. Alternatively, it can be assumed that there is a tether retraction mechanism at the base, that can remove the remaining slack from the tether when it is not used at its maximum length l . Using any of the two assumptions, a tether configuration can be expressed as one of the locally shortest paths from the tether base to robot's location. An illustration of a tethered robot in a 2D environment with obstacles is given in Figure 14.

As observed in Figure 14, being tethered to a fixed base constrains the workspace of the robot, which could otherwise contain the entire environment. The region colored in green contains the points that are within a radius of l to the base, where the white colored region lies out of the workspace of the robot. Obstacles in the environment, constrain the workspace even further for a tethered robot (from the green colored region to the shaded one surrounded by the blue dashed lines), as the tether is not expected to go through the obstacles and it

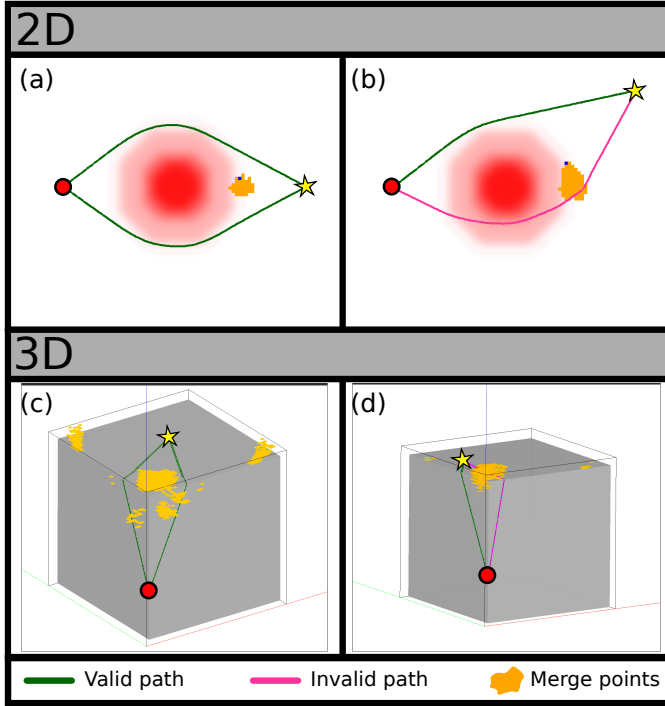


Fig. 12: **Results:** (a) Two valid paths around a small hill, when the start and goal are placed symmetrically. (b) A valid and an invalid path around a small hill, with start and goal placed asymmetrically. Invalid path goes around (touches) the artificial cut (merge points). (c) Two valid paths around the corner of a prism, when the start and goal are placed symmetrically. (d) A valid and an invalid path around the corner, with start and goal placed asymmetrically. Invalid path goes around the artificial cut introduced by the merge points.

has to be stretched longer around the obstacle. As seen around the smaller obstacle, there also exist points in the environment which can be reached via different tether configurations within the length constraint.

B. Solution

In prior work we developed a method for computing shortest traversible path in a planar, Euclidean domain with obstacles for a tethered robot with cable length constraint using a topological path planning (homotopy-augmented graph) method [25]. This approach, however, cannot be naturally extended to 3D domains since in spatial domains with obstacle there may exist locally-optimal paths that belong to the same homotopy class, but need to be made distinction between because a cable with length constraint cannot be continuously deformed from one topo-geometric class to another. Even for different topological classes, computation of homotopy invariants is extremely difficult in spatial domains [20]. Equipped with neighborhood-augmented graph for topo-geometric path planning, we can now compute optimal traversible path for a tethered robot with cable length constrain in complex spatial domains.

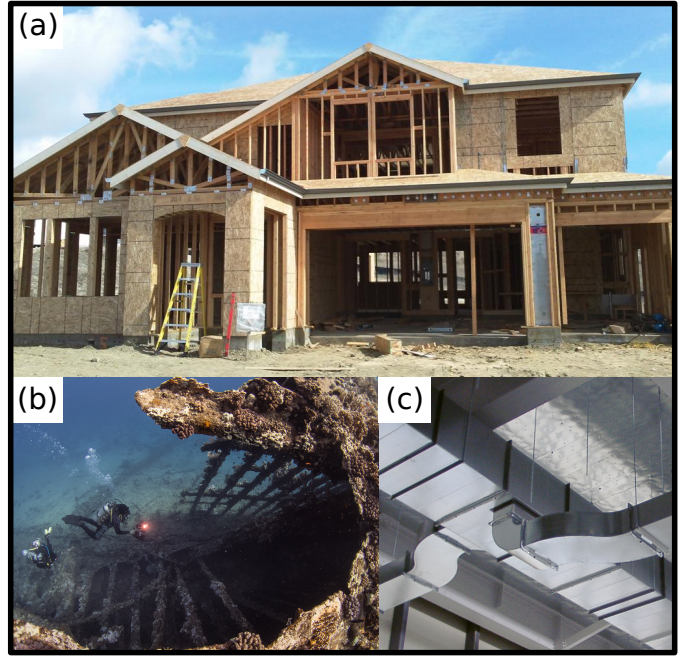


Fig. 13: (a) Building with windows (can be generalized as a genus- n object), (b) An underwater ship wreck. (c) HVAC ductwork. [Image Courtesy of Wikimedia commons.]

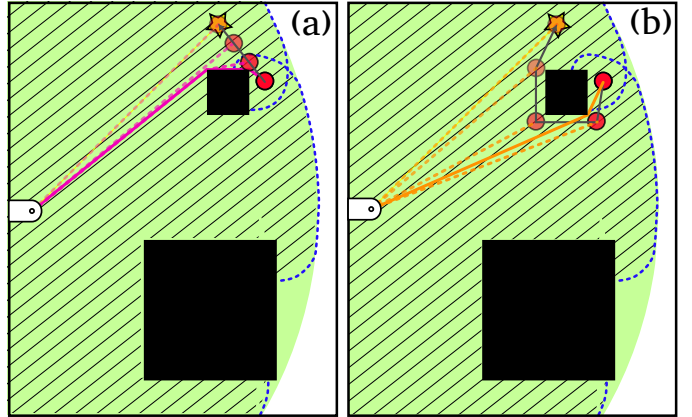


Fig. 14: (a) Tethered robot starts from an initial configuration and reaches the goal via the *globally shortest* length constrained path. (b) Robot starts from at the same coordinates but with a different tether configuration. It reaches the same goal via another length constrained path that is *locally shortest*.

Path planning for a tethered robot consists of two stages of search using neighborhood augmented graphs. The first stage is referred to as *workspace exploration*, where a neighborhood augmented graph is incrementally constructed starting from a base vertex v_b to each point in the environment that is reachable within the tether length constraint. The algorithm used for *workspace exploration* is identical to the one in Algorithm 1, where the stopping criteria is a radius based one. Instead of stopping at a vertex that has matching coordinates with the assigned goal, *workspace exploration* terminates at

the first vertex that has a g-score exceeding the maximum cable length (the stopping criterion is $g(v) < l$, similar to the one in the *computeTNS* routine given in Algorithm 3). During the construction of this fixed length graph, we use the SStar algorithm, such that the computed g-scores represent the lengths of the shortest paths in the underlying configuration space.

The second stage is referred to as *length constrained search (LCS)*, where another search is performed on the previously constructed neighborhood augmented graph. This search starts from an initial vertex v_s (note that on a neighborhood augmented graph there could exist multiple vertices with identical coordinates, but with distinct neighborhoods), which also corresponds to a unique tether configuration in the neighborhood augmented graph, and terminates at a goal coordinate q_g . In this case, there are no topological or geometrical constraints on the final tether configuration placed within the search algorithm, thus any vertex v that has matching coordinates with q_g is a valid goal vertex and any corresponding tether configuration is valid. However, as observed in Figure 14, the shape of the workspace dictates itself during the *LCS* as it is performed on the graph of the explored workspace, thus some of the goal coordinates might only be reached via certain tether configurations. Path resulting from a *LCS* is referred to as *length constrained path (LCP)* and is a locally shortest path between the start and the goal coordinates that satisfies the tether length constraint. It must be emphasized that the *LCP* obtained using this method is the globally optimal path among all the alternative paths that satisfy the tether length constraint, but it may be only locally optimal in the unconstrained configuration space.

C. Tether Length Analysis

To demonstrate the effect of the tether length constraint on the paths obtained by the length constrained search algorithm we consider a building-like environment shown in Figure 15. The building has a total of 3 rooms, where the first room on the left spans two floors and remaining two rooms are on the right connected via a hole in between. Both rooms on the right connect to the first room via doors. The first room and the room at bottom right are accessible from outside via windows. Robot is tethered to a base fixed outside and initially positioned inside the bottom right room, which it accessed through the corresponding window. The goal is placed within the first room near the window.

Keeping the initial and goal configurations the same, the length constrained search algorithm is run with varying maximum tether length l . As observed in Figure 15, *LCS* algorithm outputs the shortest path between the start and goal that would satisfy the tether length constraint. For relatively optimistic/relaxed constraints, resulting path might correspond to the globally shortest path in a given environment. With stricter constraints, the algorithm is still able to find a path between the start and goal. However, these paths might be significantly longer, requiring the robot to exit the building through the windows that it has already used while entering.

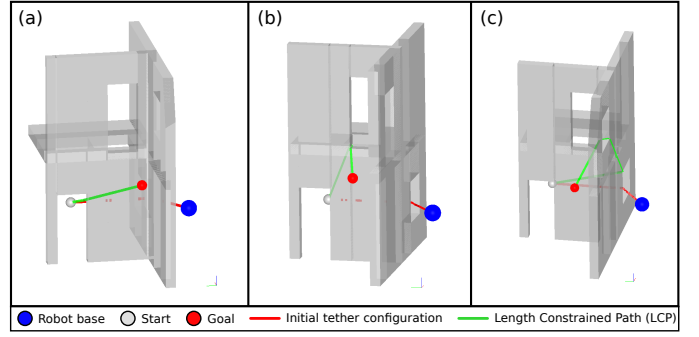


Fig. 15: **Results:** (a) Max. tether length = 30. Globally shortest path in the environment satisfies the tether length constraint. (b) Max. tether length = 25. With a shorter tether, robot has to follow the next locally shortest path (which is the second globally shortest path in the environment). (c) Max. tether length = 20. With a stricter constraint on the tether length, the path that the robot has to follow is significantly longer.

D. Simulations

We demonstrate the capabilities of the proposed *LCS* algorithm on virtual environments shown in Figure 16. In the scenario shown in Figure 16(a), there exists a long rectangular prism in the environment around which paths would be topologically equivalent but geometrically distinct. The robot is to start from an initial position and a corresponding tether configuration such that the globally shortest path from the start to goal does not satisfy the tether length constraint. The *LCP* obtained from the algorithm is shown using the green line and the sequence of tether configurations are shown using the transparent red lines. As expected, the *LCP* makes the robot move towards its base and go around the other side of the prism. It must be noted that in this scenario the path planning takes place around a genus-0 prism, which was described amongst limiting cases in the previous sections. The difference is that beyond a certain ratio of the length, width and depth of a prism, it is possible to rely on the proposed algorithm to make a geometrical distinction across the faces instead of the corners of the prism.

A similar behavior is observed in Figure 16(b), where the robot has to exit the building-like structure and use the alternative entrance instead of taking the globally shortest path to reach the goal. Figure 16(c) features a trefoil knot shaped obstacle around which a robot is to navigate between a series of goal points. In this scenario, the robot follows the globally shortest paths whenever they satisfy the tether length constraint and uses the alternative locally shortest paths when necessary.

E. Real Robot Experiments

A structure similar to the one shown in Figure 16(b) is constructed using styrofoam blocks for real robot demonstrations. Crazyflie 2.1 quadrotor platform is connected to a metal hoop (that acts as a robot base) via a red wool thread (that represents the tether). The experimental setup and the navigation progress

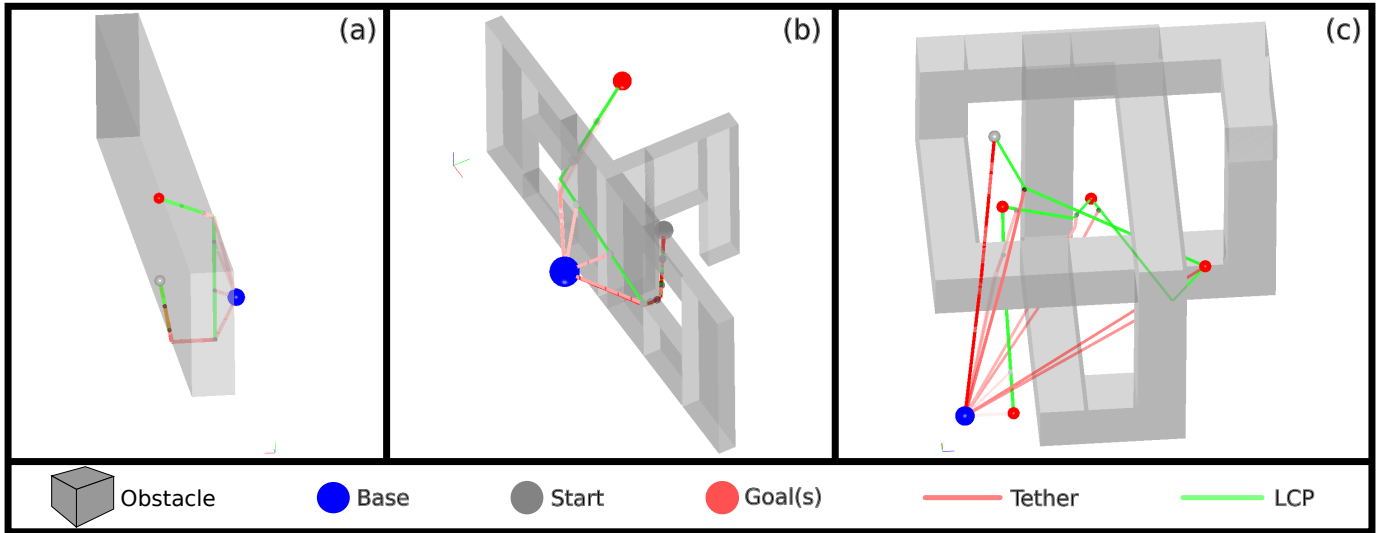


Fig. 16: **Results:** (a) Environment with long rectangular obstacle. (b) Environment with building-like structure. Building has two rooms connected via a door. Both rooms have window access and the robot base is placed outside. (c) Environment with a trefoil knot shaped obstacle. Sequence of tether configurations are plotted starting from opaque to transparent red to highlight the order.

is to be seen in Figure 17. The quadrotor is initially placed on the ground closer to the window on the left. The first goal is defined inside the room on the left which is accessed via the window as shown in Figure 17 - Step 2 and 3. The second goal is defined inside the room on the right. As shown in Steps 4-6, the quadrotor has to exit the structure and use the window on the right to reach the goal without violating the tether length constraint.

VI. CONCLUSIONS

We present a topo-geometric path-planning approach for finding multiple, locally optimal and geometrically distinct paths. This is accomplished by constructing neighborhood augmented graphs in which every vertex is identified via a neighborhood around the path leading up to that vertex. Existing graph-search algorithms can be run on these graphs to generate desired number of paths. Our method is general in the sense that it provides a way to compute multiple locally optimal paths in configuration spaces of various geometry and dimension without requiring any additional procedures. Unlike existing topological path planning methods, it is also able to find locally optimal paths that are homotopic but geometrically different.

Path planning capabilities of the algorithm are demonstrated on a variety of environments and scenarios. We further discussed the limitations of the proposed approach in low curvature environments and present modifications to the algorithm to increase path planning capabilities in these type of environments. Lastly, we implement neighborhood-augmented planning algorithm for a length constrained path planning problem. For a tethered robot navigating in 3D, we find optimal paths that satisfy the tether length constraints which we demonstrate using simulations and real robot experiments.

ACKNOWLEDGMENTS

This material is based upon work supported by the National Science Foundation under Grant No. CCF-2144246.

REFERENCES

- [1] D. Ferguson, C. R. Baker, M. Likhachev, and J. M. Dolan, "A reasoning framework for autonomous urban driving," in *Proceedings of the IEEE Intelligent Vehicles Symposium (IV 2008)*, Eindhoven, Netherlands, June 2008, pp. 775–780.
- [2] D. W. Hong, S. Kimmel, R. Boehling, N. Camoriano, W. Cardwell, G. Jannaman, A. Purcell, D. Ross, and E. Russel, "Development of a Semi-Autonomous Vehicle Operable by the Visually Impaired," *Multisensor Fusion and Integration for Intelligent Systems*, pp. 455–467, 2009.
- [3] B. Cohen, S. Chitta, and M. Likhachev, "Search-based planning for manipulation with motion primitives," in *Proceedings of the IEEE International Conference on Robotics and Automation (ICRA)*, 2010.
- [4] S. Swaminathan, M. Phillips, and M. Likhachev, "Planning for multi-agent teams with leader switching," in *ICRA*. IEEE, 2015, pp. 5403–5410.
- [5] E. W. Dijkstra, "A note on two problems in connexion with graphs," *Numerische Mathematik*, vol. 1, pp. 269–271, 1959.
- [6] P. E. Hart, N. J. Nilsson, and B. Raphael, "A formal basis for the heuristic determination of minimum cost paths," *IEEE Transactions on Systems, Science, and Cybernetics*, vol. SSC-4, no. 2, pp. 100–107, 1968.
- [7] A. Stentz, "The focussed D* algorithm for real-time replanning," in *Proceedings of the International Joint*

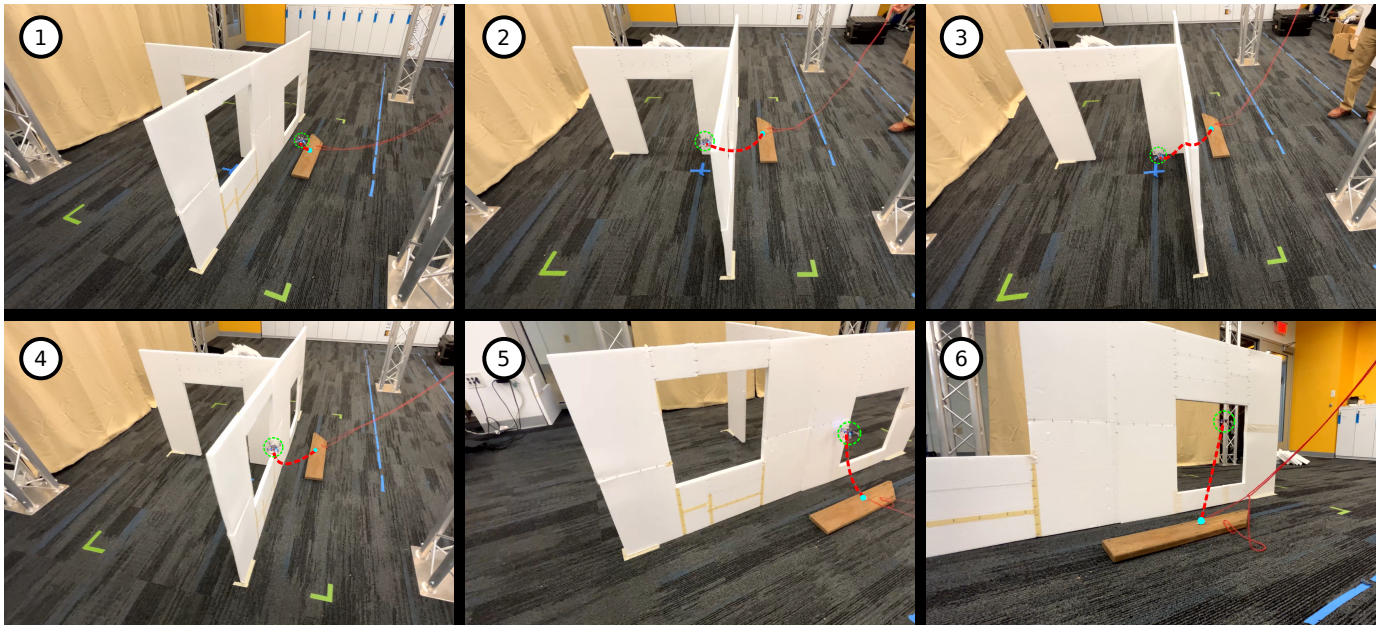


Fig. 17: Photos from real robot experiments for scenario 1a. Steps 1 through 6. Quadrotor, wool tether and robot base are highlighted with colored lines for improved visibility.

- Conference on Artificial Intelligence (IJCAI)*, 1995, pp. 1652–1659.
- [8] L. E. Kavraki, P. Svestka, J. C. Latombe, and M. H. Overmars, “Probabilistic roadmaps for path planning in high-dimensional configuration spaces,” *IEEE Transactions on Robotics and Automation*, vol. 12, no. 4, pp. 566–580, Aug 1996.
 - [9] S. M. LaValle and J. James J. Kuffner, “Randomized kinodynamic planning,” *The International Journal of Robotics Research*, vol. 20, no. 5, pp. 378–400, 2001.
 - [10] K. Daniel, A. Nash, S. Koenig, and A. Felner, “Theta*: Any-angle path planning on grids,” *Journal of Artificial Intelligence Research*, vol. 39, pp. 533–579, 2010.
 - [11] M. Cui, D. D. Harabor, and A. Grastien, “Compromise-free pathfinding on a navigation mesh,” in *Proceedings of the Twenty-Sixth International Joint Conference on Artificial Intelligence, IJCAI 2017, Melbourne, Australia, August 19-25, 2017*, 2017, pp. 496–502. [Online]. Available: <https://doi.org/10.24963/ijcai.2017/70>
 - [12] S. Bhattacharya, “Towards optimal path computation in a simplicial complex,” *International Journal of Robotics Research (IJRR)*, vol. 38, no. 8, pp. 981–1009, June 2019, doi: 10.1177/0278364919855422.
 - [13] S. Kim, S. Bhattacharya, and V. Kumar, “Path planning for a tethered mobile robot,” in *Proceedings of IEEE International Conference on Robotics and Automation (ICRA)*, Hong Kong, China, May 31 - June 7 2014.
 - [14] S. Bhattacharya, S. Kim, H. Heidarsson, G. Sukhatme, and V. Kumar, “A topological approach to using cables to separate and manipulate sets of objects,” *International Journal of Robotics Research*, vol. 34, no. 6, pp. 799–815, April 2015, doi: 10.1177/0278364914562236.
 - [15] X. Wang and S. Bhattacharya, “A topological approach to workspace and motion planning for a cable-controlled robot in cluttered environments,” *IEEE Robotics and Automation Letters*, vol. 3, no. 3, pp. 2600–2607, July 2018.
 - [16] V. Govindarajan, S. Bhattacharya, and V. Kumar, “Human-robot collaborative topological exploration for search and rescue applications,” in *International Symposium on Distributed Autonomous Robotic Systems (DARS)*, 2014.
 - [17] S. Kim, S. Bhattacharya, R. Ghrist, and V. Kumar, “Topological exploration of unknown and partially known environments,” in *Proceedings of the IEEE/RSJ International Conference on Intelligent Robots and Systems (IROS)*, Tokyo, Japan, November 3-7 2013, [DOI: 10.1109/IROS.2013.6696907].
 - [18] S. B. Xiaolong Wang, Alp Sahin, “Coordination-free multi-robot path planning for congestion reduction using topological reasoning,” 2022, arXiv:2205.00955 [cs.RO].
 - [19] S. Bhattacharya, M. Likhachev, and V. Kumar, “Topological constraints in search-based robot path planning,” *Autonomous Robots*, pp. 1–18, June 2012, doi: 10.1007/s10514-012-9304-1.
 - [20] S. Bhattacharya and R. Ghrist, “Path homotopy invariants and their application to optimal trajectory planning,” *Annals of Mathematics and Artificial Intelligence*, vol. 84, no. 3-4, pp. 139–160, December 2018.
 - [21] S. Bhattacharya, R. Ghrist, and V. Kumar, “Persistent homology for path planning in uncertain environments,” *IEEE Transactions on Robotics (T-RO)*, vol. 31, no. 3, pp. 578–590, March 2015, doi: 10.1109/TRO.2015.2412051.

- [22] M. Gromov, M. Katz, P. Pansu, and S. Semmes, *Metric structures for Riemannian and non-Riemannian spaces*. Springer, 1999, vol. 152.
- [23] M. P. Do Carmo and J. Flaherty Francis, *Riemannian geometry*. Springer, 1992, vol. 6.
- [24] S. Bhattacharya and R. Ghrist, “Path homotopy invariants and their application to optimal trajectory planning,” *Annals of Mathematics and Artificial Intelligence*, vol. 84, no. 3, pp. 139–160, 2018.
- [25] S. Kim, S. Bhattacharya, and V. Kumar, “Path planning for a tethered mobile robot,” in *2014 IEEE International Conference on Robotics and Automation (ICRA)*, 2014, pp. 1132–1139.